Two-phase flow patterns in adiabatic and diabatic corrugated plate gaps

Two-phase flow patterns in adiabatic and diabatic corrugated plate gaps

A.-E. Polzin[1*], S. Kabelac[1], B. de Vries[2]
[1]Institute for Thermodynamics, Leibniz University Hannover, Germany
[2]Kelvion PHE GmbH, Sarstedt, Germany

*E-mail: polzin@ift.uni-hannover.de

Abstract. Correlations for two-phase heat transfer and pressure drop can be improved considerably, when they are adapted to specific flow patterns. As plate heat exchangers find increasing application as evaporators and condensers, there is a need for flow pattern maps for corrugated plate gaps. This contribution presents experimental results on flow pattern investigations for such a plate heat exchanger background, using an adiabatic visualisation setup as well as a diabatic setup.
Three characteristic flow patterns were observed in the considered range of two-phase flow: bubbly flow, film flow and slug flow. The occurrence of these flow patterns is a function of mass flux, void fraction, fluid properties and plate geometry. Two different plate geometries having a corrugation angle of 27° and 63°, respectively and two different fluids (water/air and R365mfc liquid/vapor) have been analysed. A flow pattern map using the momentum flux is presented.

1. Introduction

Due to their advantages like high compactness and high flexibility together with high heat transfer characteristics, plate heat exchangers (PHEs) find broad application in many industrial fields. For single-phase applications, reliable models for the flow distribution as well as the heat transfer and pressure drop characteristics are available, e.g. [1], [5].

Today, PHEs are also frequently used for two-phase applications, where the working fluid evaporates or condenses, although no consistent models for the thermodynamic and hydraulic design of apparatuses with phase change situations are available. Previously published design correlations on that topic are highly empirical and fitted to very restricted data sets only.

For an efficient design and operation of PHEs as condensers and evaporators and their optimized integration in technical plants, suitable correlations are required. Therefore, the phenomenological relation between two-phase flow, heat transfer and pressure drop behavior, which all affect each other, needs further investigation. This leads to the objective of the present study, which aims to develop a phenomenological model for two-phase heat transfer and pressure drop in PHEs. The chosen procedure is shown schematically in Figure 1. Experimental results of an adiabatic as well as a diabatic visualization setup are evaluated in terms of local heat transfer and frictional pressure drop and are brought together with experimentally gained data of a compression refrigeration cycle in technical scale, where condenser and evaporator are designed as PHEs. Additionally, a broad literature database is built and continuously maintained. Based on the own experimental data together with the experimental data on PHEs from the database, a reliable model can be developed with a validity over a large range of operation conditions, accounting for different plate geometries and fluids.

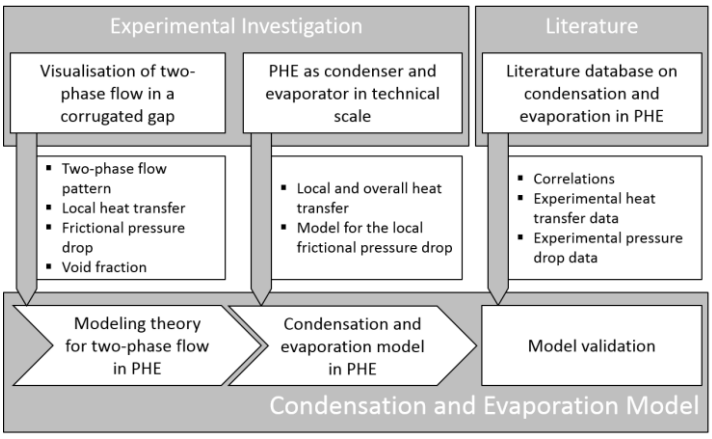

Figure 1. Procedure for the development of a phenomenological model for condensation and evaporation in PHEs

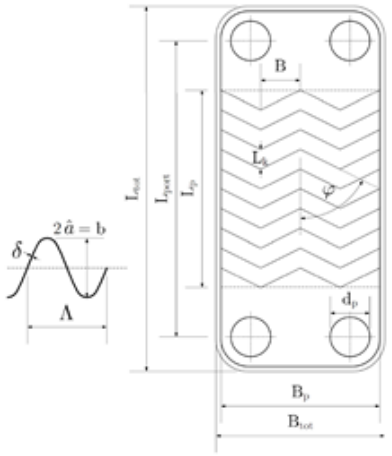

Figure 2. Geometric characteristics of a double-herringbone chevron plate [3]

A typical chevron plate with double-herringbone corrugation is depicted in Figure 2. The corrugation angle φ is taken relative to the main direction of flow. The hydraulic diameter is calculated as

$$d_h = 2b/\phi \quad (1)$$

where ϕ is the enlargement factor and b the corrugation depth.

In the following chapter 2, an overview on recent publications on flow pattern investigations in PHEs is given. Subsequently, the experimental setups und procedures, used in this work, are described. The results are presented and discussed in chapter 4. Finally, the paper is summarized and conclusions are drawn.

2. Literature

Two-phase flow patterns in PHEs have been investigated by several researchers. In the following, recent publications on two-phase flow patterns in PHEs are presented.

Tribbe and Müller-Steinhagen [7] observed air-water two-phase flow patterns in a transparent adiabatic corrugated gap with different corrugated plate pairings (30°/30°, 60°/60° and 30°/60°). Flow pattern maps were compiled with the experimental data. A correlation for the two-phase multiplier as a function of the Lockhart-Martinelli parameter was fitted to the experimental data.

Winkelmann [10] used a PHE with transparent front plate and a corrugation angle of 25.7° to examine the air and water two-phase flow in the corrugated gap. Pressure measurements were taken at the beginning and the end of the main section of the plate. From the experimental results, a two-phase multiplier correlation was derived.

Two-phase flow and pressure drop characteristics of air-water flow in a single pass PHE with asymmetric corrugated plates were studied experimentally by Nilpueng and Wongwises [6]. With a transparent front plate vertical upward and downward flow could be visualized. Flow pattern maps were conducted with the observed flow patterns for the upward and downward flow. The superficial velocity was taken as characteristic variable. Based on the experimental pressure drop measurements, they derived a correlation for the two-phase multiplier. The correlation predicts the two-phase pressure drop with a mean deviation of 12,7 %. Because of the custom-built corrugation of the plates, the results for flow pattern and pressure drop cannot be transferred directly to symmetrically corrugated PHEs.

Vakili-Farahani et al. [8], [9] investigated flow bowling and two-phase flow of R245A in a PHE. They analyzed the adiabatic pressure drop ([9]) as well as the boiling heat transfer ([8]). With an infrared camera the temperature of the front stainless steel plate was measured. These measured wall temperatures were assumed to be equivalent to the fluid temperature inside the gap. For the adiabatic

situation, they postulated the fluid to be in a saturated state within the PHE. Therefore, the determined fluid temperature would imply the fluid's saturation pressure. The described approach led to a local pressure distribution of the two-phase fluid flow within the corrugated gap of the PHE. For the diabatic setup, local heat transfer coefficients were determined with the local fluid temperatures calculated from the pressure drop analysis, conducted in [9], and the wall temperatures, measured with the IR camera.

Koyama et al. [4] investigated flow boiling of Perfluorohexan in a PHE with a transparent cover plate for parallal and counter flow. The Titanium plates did not exhibit a macroscopic corrugation but had a micro pin-fin structure on the evaporation surface. They observed three different flow patterns during evaporation along the plate: bubbly flow, slug flow, and churn flow. The determined overall heat transfer coefficients were higher for the parallel flow arrangement.

3. Experimental setup and procedures

In this paper, the focus lies on the flow pattern investigations in a corrugated plate gap. Therefore, in the following chapter, the two experimental setups, which were used to conduct the investigations, will be presented.

3.1. Adiabatic corrugated gap

The test section for the two-phase flow visualisation in an adiabatic corrugated gap is shown in Figure 3. The gap is formed by two transparent polyurethane plates, which were casted from industrial steel plates with typical corrugation. The geometric parameters of the plate's corrugation and the setup are summarized in Table 2. The inlet areas were cut off from the original plate geometry (as seen in Figure 2). By only replicating the main section, special mixing manifolds can be used together with the inlet and outlet manifold in order to assure even distribution of gaseous and liquid flow over the gap width.

Figure 3. Transparent corrugated adiabatic test section (corrugation angle of 27°)

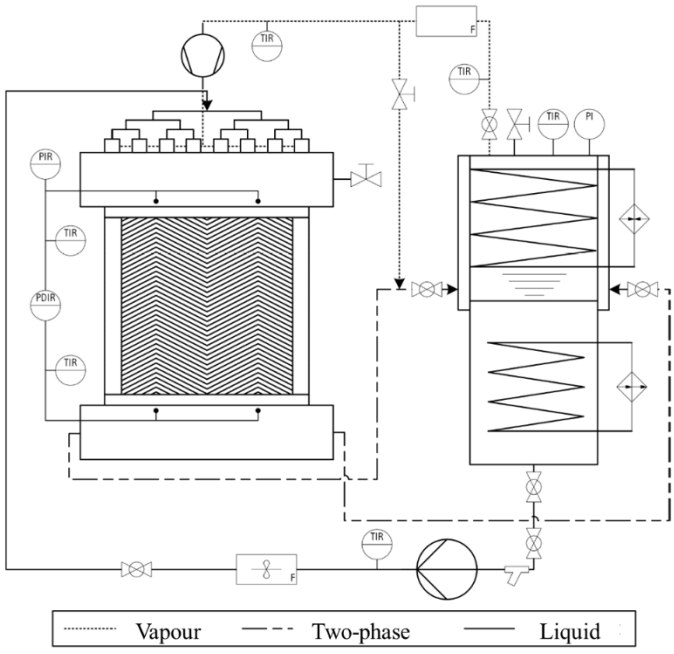

Figure 4. Schematic flowsheet of the adiabatic test facility with test section (left) and refrigerant tank (right)

Figure 4 depicts the flowsheet of the test facility, in which the transparent test gap is embedded. The working fluid, refrigerant R365mfc (1,1,1,3,3-Pentafluorobutane) is kept in the tank at equilibrium. The characteristic properties of R365mfc are listed in Table 1. R365mfc features a relatively high normal boiling point, so that the saturation pressure at operating temperatures (30 – 40 °C) is below ambient

pressure. This assures good contact of the plates over the whole test section and leads to a better mechanical stability of the corrugated gap. In conventional PHEs this would be done by the thick frame plates of a conventional plate-and-frame heat exchanger.

From the tank, the liquid and vapor phase are lead separately to the mixing section and to the inlet manifold. The liquid flow is controlled by a pump and measured by a turbine flow meter. A controllable fan is pumping the vapor phase to the mixing section. The vapor mass flow is measured by a Coriolis flow meter. In that way, the vapor quality as well as the massflux in the test section can be adjusted precisely. Temperatures are measured at relevant positions along the setup. The pressure difference between inlet and outlet of the transparent gap is measured, as well as the absolute pressure at the inlet.

A high speed camera (Phantom v5.1) is used to record the flow patterns. The camera has a maximum resolution of 1200 frames per second and 1024 × 1024 pixels.

Table 1. Properties of refrigerant R365mfc.

Molecular formular	$C_4H_5F_5$	
Molecular mass M	148.07 g/mol	
Evaporation enthalpy $\Delta^V h(T_{NB})$	188.19 kJ/(kg·K)	
Normal boiling temperature $T_{NB,p=101.3\ kPa}$	313.3 K	
Triple point	T_{tr} = 239.0 K	p_{tr} = 2.478 kPa
Critical point	T_K = 460.0 K	p_K = 3266 kPa
Density [a]	ρ_{liquid} = 1377 kg/m³	ρ_{vapor} = 5.193 kg/m³
Viscosity [a]	η_{liquid} = 380.3 µPa·s	η_{vapor} = 9.769 µPa·s
Thermal conductivity[a]	λ_{liquid} = 0.1040 W/(m·K)	λ_{vapor} = 0.009289 W/(m·K)

[a] at p^{sat} = 100 kPa; T^{sat} = 39.83°C

3.2. Diabatic corrugated gap

For the visualization of evaporation in a corrugated PHE gap, a new test setup was built, which allows for the observation of two-phase flow pattern during boiling and condensation. The test section is shown in Figure 5 and consists of two corrugated gaps with a transparent polyurethane front plate for the visual accessibility. The front plate was manufactured by milling and polished afterwards to reach optimal transparency. Table 2 depicts the main parameters of the plate and its corrugation.

The setup consists of two fluid loops, which are fed from two separate tempered tanks. The fluid in both loops is R365mfc. This refrigerant was chosen due to the same reasons as stated in section 3.1. The evaporating fluid is pumped to the inlet manifold front gap of the test section. On its way upwards through the corrugated gap, it is partly evaporated. The two-phase flow is led from the outlet manifold back to the tank, where the fluid is cooled by a thermostat.

On the heating fluid side, a fan is used to pump the vapor phase from the tank to the inlet manifold of the heating gap. The vapor reaches the gap at saturated condition and at higher temperature compared to the evaporating fluid's temperature, so that the heating fluid is condensing inside the rear corrugated gap. A condensing fluid as heat source was chosen because of equalized temperature difference between the heating (condensing) and the cooling (evaporating) fluid.

Flow rates are measured for both fluid loops as well as temperatures and pressures at relevant positions in both cycles.

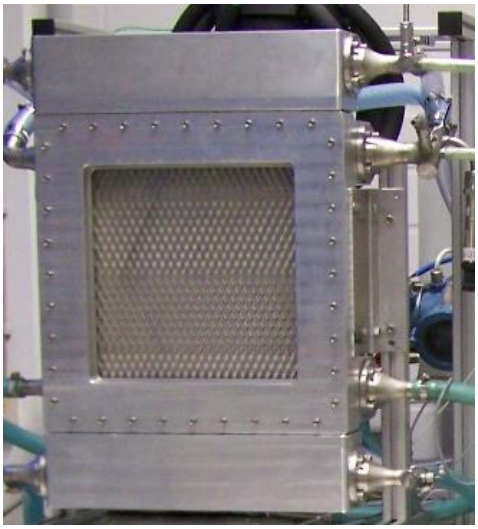

Figure 5. Test section for the diabatic experimental setup (corrugation angle of 27°)

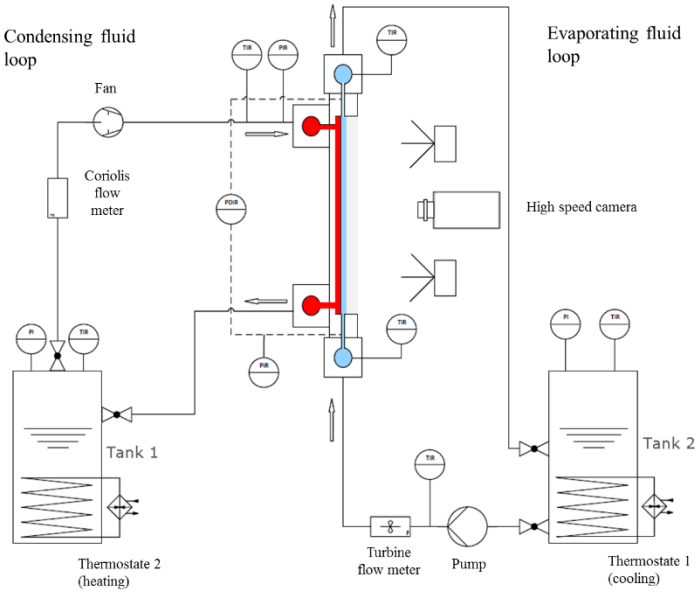

Figure 6. Schematic flowsheet of the diabatic test facility with condensing fluid loop (left) and evaporating fluid loop (right)

Table 2. Geometric parameters of the plates used in both visualization test setups

Corrugation depth b	3.0 mm
Corrugation length Λ	11.4 mm
Corrugation angle φ	27° / 63°
Corrugation width B_p	388 mm [a] / 380 mm [b]
Corrugation length L_p	408 mm [a] / 380 mm [b]
Area enlargement factor ϕ	1.155
Hydraulic diameter d_h	5.195 mm
Plate thickness s [b]	0.5 mm

[a] Adiabatic corrugated gap
[b] Diabatic corrugated gap

3.3. Data reduction

The characterization of the flow condition in the adiabatic corrugated gap is done by the momentum flux j of both phases. j is calculated as a product of superficial velocity $w_{s,i}$ and density ρ_i of the phase i ($i = V$: vapor phase, $i = L$: liquid phase):

$$j_i = w_{s,i}^2 \cdot \rho_i \tag{2}$$

$$w_{s,i} = \dot{V}_i / b \cdot B_P \tag{3}$$

where $\dot{V}_i$ is the volume flow of the phase i, b depicts the corrugation depth and B_P is the width of the corrugation.

In most previous studies (e.g. [6], [7], [10]), the superficial velocity is used to specify two-phase conditions. The use of the momentum flux as specification variable bears the advantage of a comparability between different fluids as the density is taken into account.

4. Results and discusion

In the following sections the experimental results gained with the two setups, described in the previous chapter, will be presented and discussed.

4.1. Adiabatic corrugated gap

In the considered range of momentum flux ($j_V \leq 60$ kg/(m·s²), $j_L \leq 500$ kg/(m·s²)), three main flow patterns were observed with the adiabatic corrugated gap: Bubbly flow, film flow and slug flow.

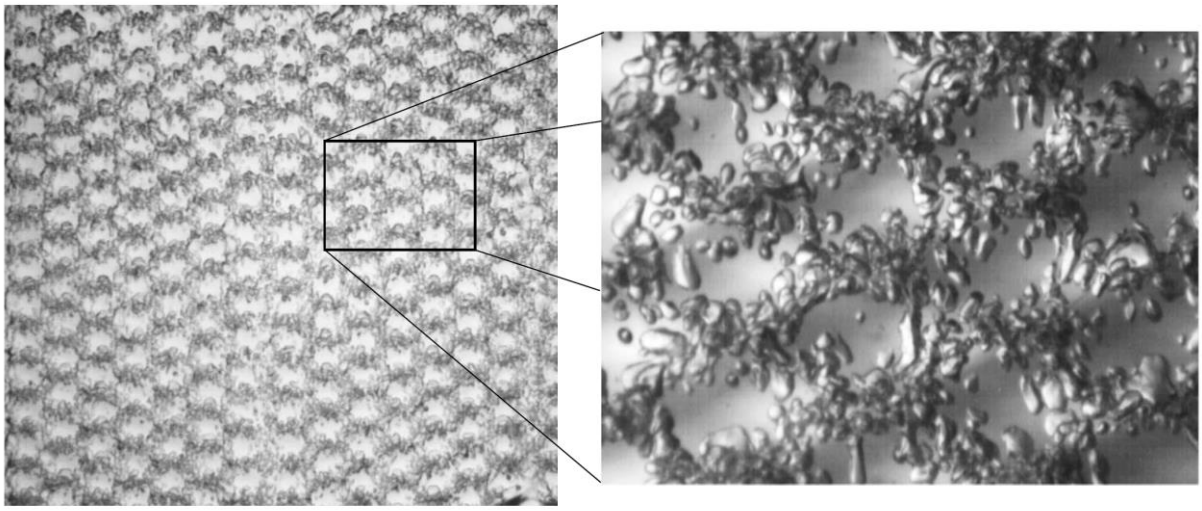

Figure 7. Bubbly flow situation of a two-phase R365mfc downward flow (corrugation angle of 63°)

A typical bubbly flow situation is shown in Figure 7. This flow pattern is characterized by small vapor bubbles, which are dispersed evenly in the liquid flow. With the bubbles, the flow path of the fluid can be observed. The two-phase flow follows the behaviour, which Focke and Knibbe [2] observed for single flow: For low Reynolds numbers, the bubbles follow the long corrugation valleys until they reach the wall, where they are deflected and moving further down among the next corrugation valley. At high Reynolds numbers the bubbles take the shorter way down which implies a lot more deflections and direction changes. The flow path can be describes as a narrow zig zag line. Bubbly flow occurs at lower vapor momentum fluxes and relatively high liquid momentum fluxes. For vapor qualities, higher than 0.015, the size of bubbles reaches the point, where some agglomerate to larger voids of gas phase, leading to irregular bubbly flow. Bubbly flow and irregular bubbly flow can be observed at a liquid momentum flux >10 kg/(m·s²) and for vapor momentum fluxes of 9 kg/(m·s²) or lower.

At high vapor momentum fluxes (> 9 kg/(m·s²)) and liquid momentum fluxes below 10 kg/(m·s²), film flow can be observed. It is characterized by a liquid film, flowing on the walls of the corrugated gap with the vapor phase flowing in the gap's centre at a higher velocity. Due to different velocities of the phases, high shear forces occur between the phases. A typical image of a film flow situation is given in Figure 8.

The third main flow pattern, slug flow, can be observed at high momentum fluxes of both phases. Figure 9 depicts a typical slug flow situation. It is characterized by alternating regions of liquid and gaseous flow dominated domains.

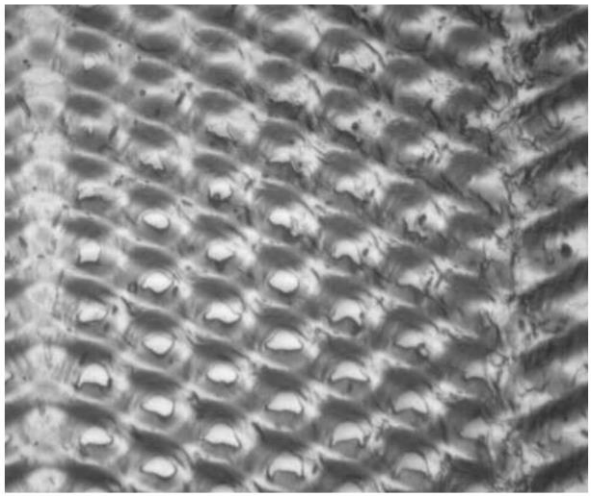

Figure 8. Film flow of a two-phase R365mfc downward flow (corrugation angle of 63°)

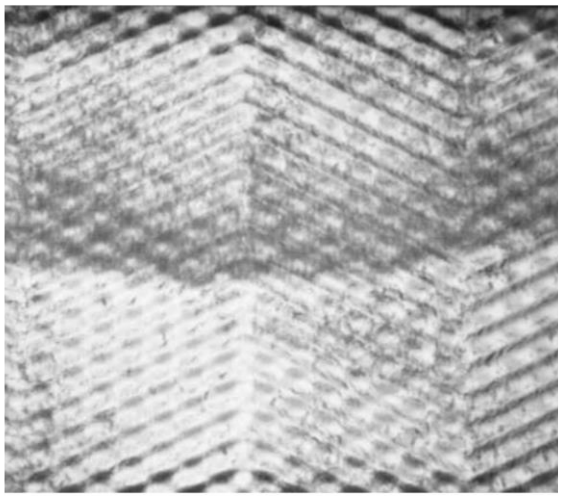

Figure 9. Slug flow of a two-phase R365mfc downward flow (corrugation angle of 63°)

The results for the flow pattern observations for two-phase downward flow in an adiabatic corrugated gap with two different corrugation angles (27° and 63°, respectively) are summarized in a flow pattern map, which is shown in Figure 10.

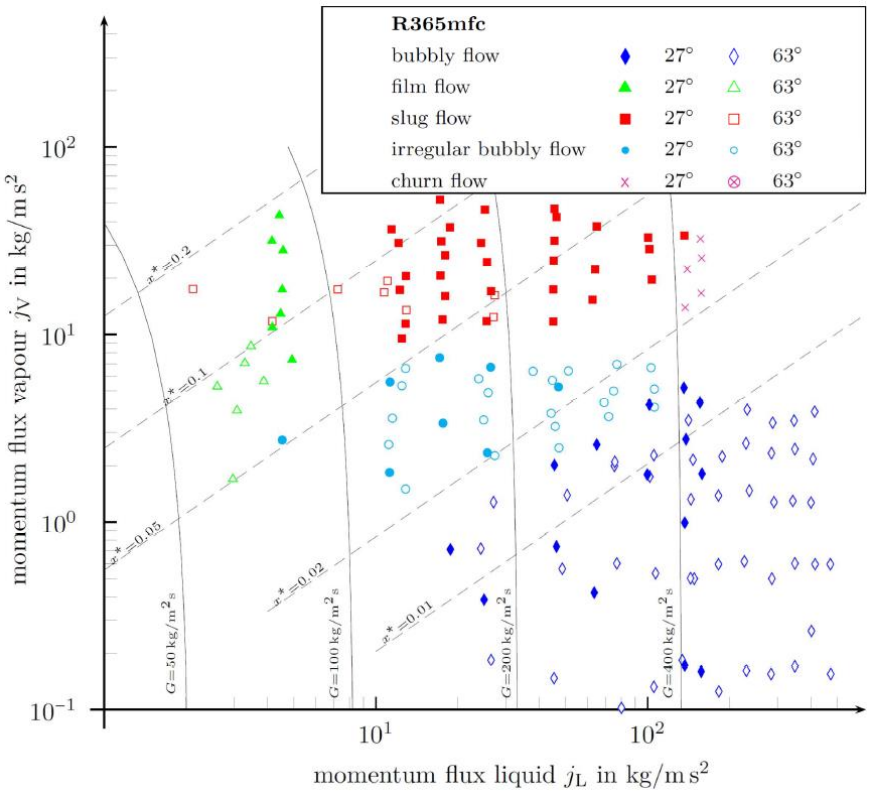

Figure 10. Flow pattern map for two-phase R365mfc downward flow in a corrugated gap with corrugation angles of 27° (solid symbols) and 63° (bordered symbols) [3]

This flow pattern map is combining the results of Grabenstein [3] and own new ones, obtained on the same experimental setup.

The dashed lines connect the points of constant vapor quality. For a phase-change situation, e.g. during condensation or evaporation, the overall fluid mass flux would stay constant, as the mass flow and the gap geometry do not change within the apparatus. Some paths of constant mass flux are therefore indicated as solid lines within the flow pattern map.

4.2. Diabatic corrugated gap

For the diabatic test setup, visualization tests with air-water flow have been conducted. To deliver high quality video and image recordings with the high speed, a sufficient lighting has to be ensured. Contrary to the adiabatic transparent gap, where the lighting can be provided from behind, through the transparent plates, the lighting in the diabatic setup has to be provided frontally. A representative image, recorded during a visualization test with air water flow with the high speed camera, is depicted in Figure 11. It can be seen, that a high quality imaging is ensured with the utilized lighting.

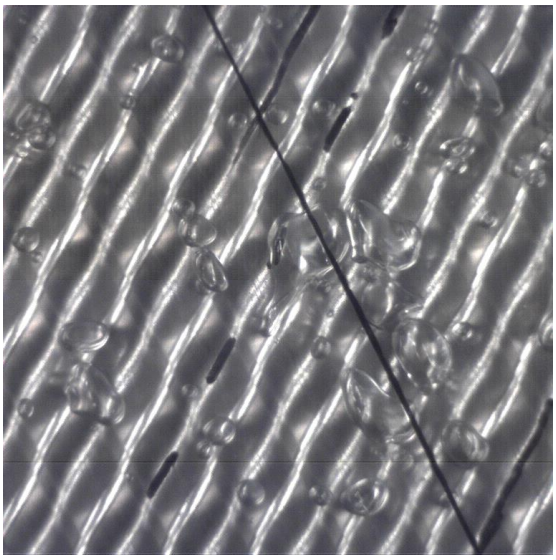

Figure 11. Two-phase air-water flow in the diabatic test setup with a corrugation angle of 27°

The dashed and solid line indicate the corrugation wave crest of the back plate and the transparent front plate, respectively. These lines give a good impression on the refraction of the polyurethane plates. It can be seen, that the image is not distorted by the refractive index of the corrugated transparent plate. Further investigations with the diabatic setup and the evaporation of R365mfc will be conducted in the close future.

5. Conclusion

Two-phase flow patterns inside a PHE have been experimentally investigated for different corrugation angles. A transparent adiabatic corrugated gap was used to visualize the two-phase flow pattern at various mass fluxes and void fractions. Three characteristic flow patterns were observed: bubbly flow, film flow and slug flow. The characterized flow patterns were plotted as a function of momentum flux of the liquid and the gaseous flow to compile a flow pattern map which is valid for various pure fluids.

First experiments have been made with a new diabatic test setup, where evaporation in a corrugated gap can be visualized. The first results show a high recording quality with a high speed camera, where the lighting requirements are met satisfyingly.

In a next step, evaporation experiments will be conducted with the newly the developed diabatic test setup.

References

[1] Bassiouny M K 1985 *Experimentelle und theoretische Untersuchungen über Mengenstromverteilung, Druckverlust und Wärmeübergang in Plattenwärmeaustauschern* PhD Thesis Karlsruhe University
[2] Focke W and Knibbe P 1986 *J. Fluid Mech.* **165** 73-77
[3] Grabenstein V 2014 *Experimental investigation and modelling of condensation in plate heat exchangers* PhD Thesis Gottfried Wilhelm Leibniz University Hannover LUH
[4] Koyama K, Nakamura Y, and Arima H 2014 *ASME 2014 International Mechanical Engineering Congress and Exposition*. American Society of Mechanical Engineers V08AT10A001-V08AT10A001
[5] Martin H ed. 2010 Pressure Drop and Heat Transfer in Plate Heat Exchangers *VDI Heat Atlas* 2nd ed. (Berlin Heidelberg: Springer-Verlag) chapter N6 pp 1515-1522
[6] Nilpueng K and Wongwises S 2010 *Exp. Therm. Fluid Sci.* **34** 1217-1229
[7] Tribbe C and Müller-Steinhagen H M 2001 *Heat transfer eng.* **22**(1), 12-21
[8] Vakili-Farahani F V, Amalfi R L and Thome J R 2014 *Int. J. Interfac. Phenom. Heat Transf* **2** 343-361
[9] Vakili-Farahani F V, Amalfi R L and Thome J R 2014 *Int. J. Interfac. Phenom. Heat Transf* **2**(4) 325-342
[10] Winkelmann D 2010 *Condensation of pure refrigerants and their zeotropic mixtures in plate heat exchangers* PhD Thesis Technical University of Berlin